Atmospheric greenhouse gas concentrations from the ice core record

Air bubbles represent ~10-15% of the volume of the ice at the bubble close-off depth

Firn-Ice Transition

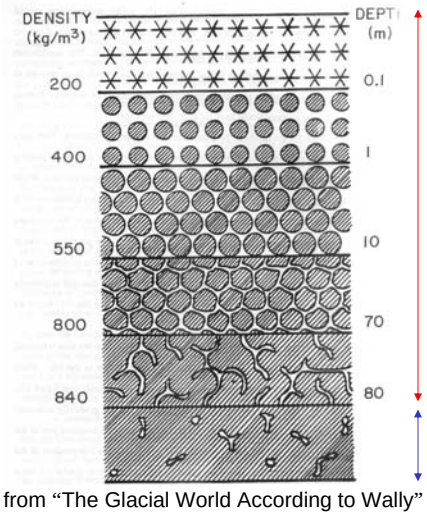

from "The Glacial World According to Wally"

Firn: porous, unconsolidated layer of snow on top of polar ice sheets (~90 m at Vostok)

Gases diffuse throughout the layer of firn and fractionate due to gravity, and temperature and concentration gradients

Ice: air bubbles are closed off due to densification of ice due to hydrostatic pressure

Close off depth depends on temperature and accumulation rate

Regimes of gas-transport in firn

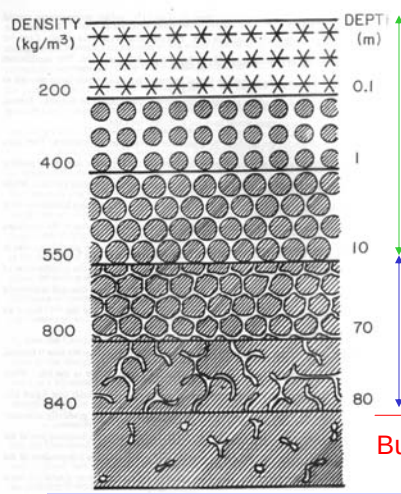

Convective mixing of air due to surface wind stress (wind pumping)

Stagnant air column – transport by molecular and atomic diffusion

Bubble close off

Both diffusion and gradual bubble close off leads to a smoothing of gas concentrations over time

The time span over which trapping occurs depends mostly on the snow accumulation rate and can vary from several years to hundreds of years.

Factors influencing the composition of air in the firn (stagnant air column)

Gravitational fractionation: the pressure of gases increases with depth below the surface so that heavier species are enriched at depth:

$$\delta = \left[\exp\left(\frac{\Delta m g z}{RT} \right) - 1 \right] 10^3$$

Δm = mass difference; g = gravitational acceleration constant; z = depth; R = ideal gas constant; T = temperature [K]

Thermal diffusion: gases diffuse faster than heat (important for rapid climate change only)

$$\delta = \left[\frac{R}{R_0} - 1 \right] 10^3 = \left(\left[\frac{T_0}{T} \right]^{\alpha} - 1 \right) 10^3$$

T, T_0 = temperature (K); α = thermal diffusion factor (characteristic of a pair of gas species)

Concentration diffusion: in response to a concentration gradient

Porosity of firn: a function of density

Gravitational Fractionation

$\delta^{15}N$ from two east Antarctic ice cores

Perfect diffusive equilibrium

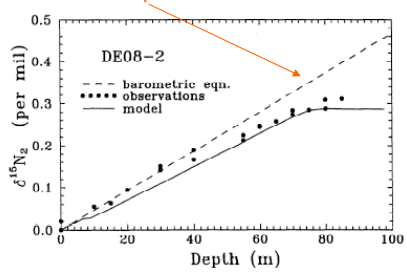

Figure 4. Observations and model calculation of $\delta^{15}N_2$ in the DE08-2 firn. The model calculation includes the 1990 melt layer (see section 7 for details).

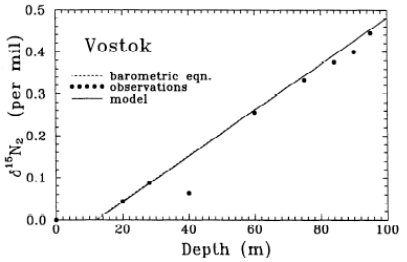

Figure 6. Model calculation of $\delta^{15}N_2$ in the Vostok firn, with observations from *Bender et al.* [1994]. The model calculation assumes that the top 13 m of firn are well mixed by convection.

Trudinger et al. [1997]

Porosity and diffusivity in firn

Δage often determined using a model for gas diffusion and bubble trapping in firn, using profiles of density, porosity, and diffusivity. These profiles can be determined by models or curves fitted from measured data.

Density is determined from temperature and accumulation rate. → Porosity = f(density) [empirical]

Diffusion = f(T, molecular weight, porosity)

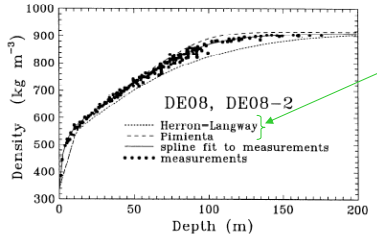

Figure 1. Density profiles for the DE08 and DE08-2 sites calculated with the Herron-Langway model and the Pimienta model, as well as measured values and a smoothing spline fit to measurements.

Models are empirically based density parameterizations

Diffusivity-porosity relationship is the most uncertain component of the gas diffusion model.

Trudinger et al. [1997]

Age distribution of gases in firn calculated from a diffusion model

Rectangular pulse in the atmosphere

Trudinger et al. [1997]

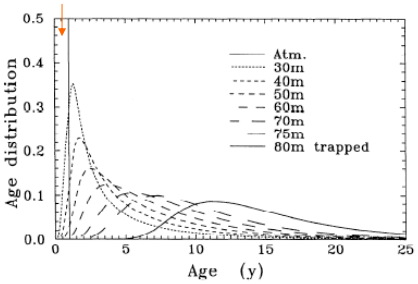

Figure 11. Age distributions of CO_2 molecules in the DE08 firn from the surface to 75 m, and in the ice at 80 m, calculated by using the diffusion model.

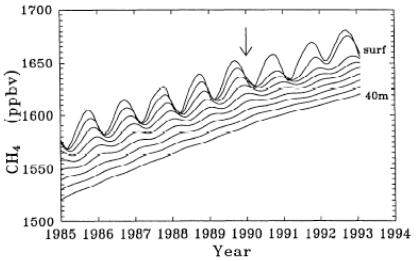

Figure 10. Time series of modeled CH_4 between the surface and 40 m at depth intervals of 5 m in the DE08-2 firn. The arrow indicates approximately when the melt layer was at the surface.

Effective age: elapsed time since the surface was at the same concentration as is currently seen at depth z

Ice-age gas-age difference estimates from $\delta^{15}N$ measurements

Limited to rapid climate changes only

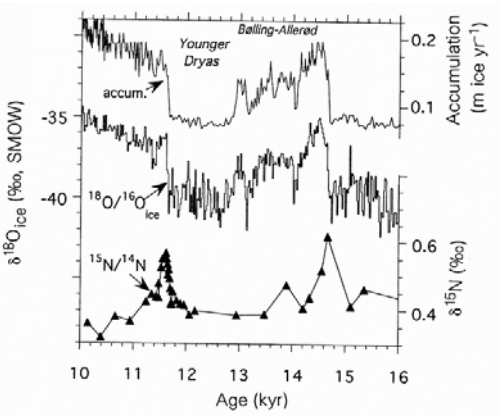

Severinghaus et al. [1998]

GRIP, Greenland

Dependence of linear correlation coefficient (r^2) on 2 temperature proxies, $\delta^{18}O_{ice}$ and $\delta^{15}N$, on the mean Δage (7800-8780 y B.P.)

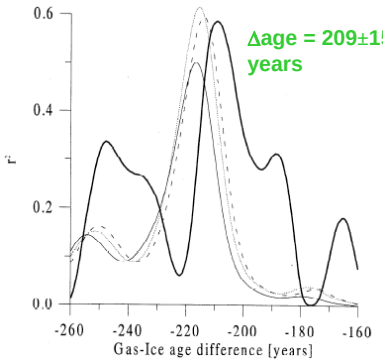

Leuenberger et al. [1999]

Ice-age gas-age difference estimates from $\delta^{40}Ar$ measurements

Vostok, Antarctica

Δage = 4100 $\pm$ 250 years

(240,000 y B.P.)

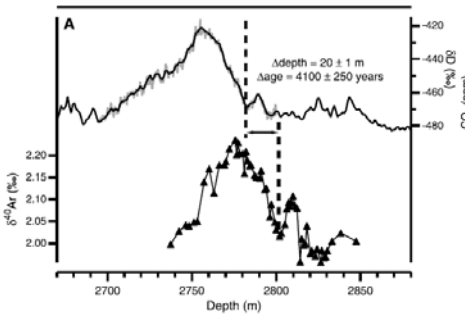

CO_2 lags temperature increase by 800 $\pm$ 200 years

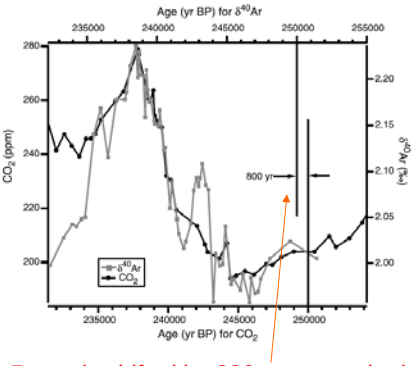

Records shifted by 800 years to obtain best correlation between two data sets

Caillon et al., 2003

Preservation of CO_2 in Greenland Ice

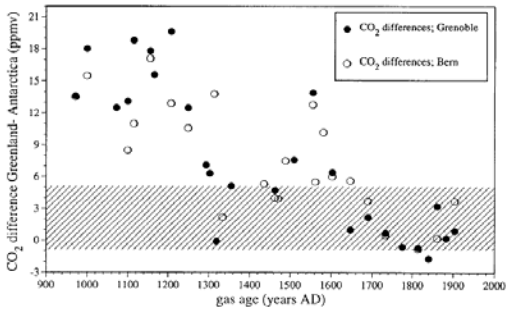

Anklin et al. [1995]

Fig. 3. Differences between CO_2 results obtained from Greenland (Eurocore, GRIP) and Antarctic ice cores (South Pole, D47, D57). The hatched area (CO_2 differences between -1 and 5 ppmv) indicates the range of CO_2 differences, which can be explained by the inter-hemispheric gradient.

Chemical production of CO_2 below the bubble close off depth likely due to reactions between carbonate and acidity in liquid-like layers between grain boundaries in polar ice. Estimated concentrations of carbonate in Greenland ice is about an order of magnitude greater than in Antarctic ice. The excess CO_2 concentration in Antarctic ice from this process would be in the range of the error of a single CO_2 measurements (±3 ppmv) or less.

Analytical techniques for measuring gases trapped in ice cores

Wet Technique

Insert ice sample into an extraction vessel

Evacuate vessel

Allow the ice to melt and refreeze in vacuo to liberate trapped gases

Used to analyze gases that are relatively insoluble and chemically stable in water (CH_4, N_2, O_2, Ar)

Extraction efficiency >99%

Cannot be used for CO_2 due to reactions between carbonate dust particles and acidic aerosols in the liquid phase

Dry Technique

Insert sample into stainless steel extraction vessel

Evacuate vessel

Crush, grate, or mill ice sample into very small pieces to liberate occluded air

Extraction efficiency <80%

±0.38% for CO_2

Sublimation Technique

Insert sample into glass extraction vessel

Evacuate vessel

Apply infrared light to heat the ice to a temperature just below the melting point

Water vapor and air is cryogenically removed

Extraction efficiency >99%

±2% for CH_4 (all techniques), ±3% for N_2O

CO_2 and CH_4 measured using gas chromatography

Sowers et al. [1997]

Advantages/disadvantages of measuring greenhouse gas concentrations in ice core gas bubbles

Advantages:

Provides "direct" samples of ancient air throughout the ice core record (~800,000 years)

Provides by far the best information available on paleo greenhouse gas concentrations

Long residence times of greenhouse gases (10-100 years), compared to short mixing time of atmosphere (1 year), makes measurement at one location (Greenland or Antarctica) representative of global conditions

Disadvantages:

Must determine gas-age ice-age difference in order to date samples. Δage varies from several to thousands of years. Uncertainty as high as >1,000 years in deeper records. Gas-age ice-age difference will vary with time (due to changes in T, accumulation rate)

Gradual bubble close off during the transition from firn to ice leads to a smoothing of atmospheric concentrations over time.

Recent trends in CO_2, CH_4, and N_2O

DE 08 Antarctica core (Δage ~ 30 years)

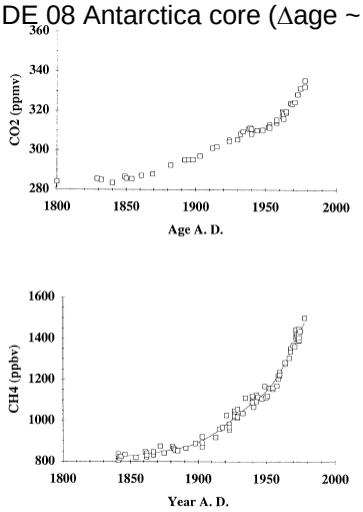

FIG. 3. (*Upper*) CO_2 vs. time before present, as inferred by Etheridge *et al.* (17) from ice core studies. (*Lower*) CH_4 vs. time before present, as inferred by Etheridge *et al.* (19) from ice core studies.

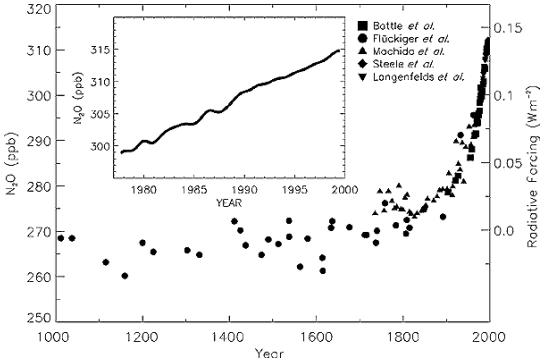

IPCC [2001]

Bender et al., 1997

CO_2 from the EPICA (Antarctica) ice core

Fig. 4. A composite CO_2 record over six and a half ice age cycles, back to 650,000 years B.P. The record results from the combination of CO_2 data from three Antarctic ice cores: Dome C (black), 0 to 22 kyr B.P. (*9*, *11*) and 390 to 650 kyr B.P. [this work including data from 31 depth intervals over termination V of (*1*)]; Vostok (blue), 0 to 420 kyr B.P. (*5*, *7*), and Taylor Dome (light green), 20 to 62 yr B.P. (*8*). Black line indicates δD from Dome C, 0 to 400 kyr B.P. (*1*) and 400 to 650 kyr B.P. (*18*). Blue line indicates δD from Vostok, 0 to 420 kyr B.P. (*7*).

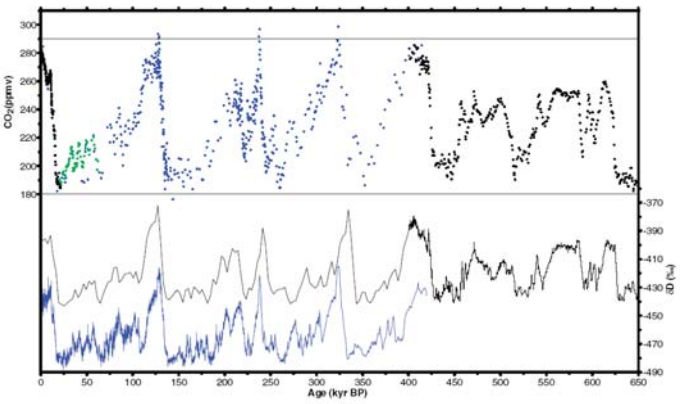

Siegenthaler et al., 2005

CH_4 and N_2O from the EPICA (Antarctica) ice core

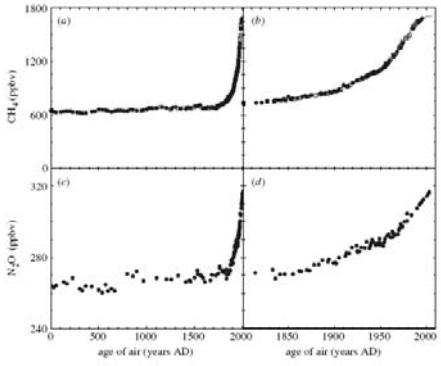

Figure 1. (a, b) CH_4 (on the CSIRO calibration scale) and (c, d) N_2O concentrations over the last (a 2000 years and (b, d) 200 years, based on measurements from firn air and ice at Law Dome, Antarct (MacFarling Meure *et al.* 2006). Black circles are from MacFarling Meure *et al.* (2006); open squa are from Etheridge *et al.* (1998); the line (CH_4) and the black triangles (N_2O) are annual averages o flasks collected at Cape Grim Observatory, Tasmania.

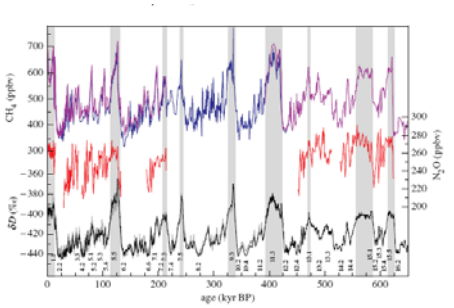

Figure 2. CH_4 and N_2O records over the last 650 kyr (Spahni *et al.* 2005 and references therein), based on data from Dome C (CH_4, purple line; N_2O, red line; excluding data believed to contain artefact) and Vostok (CH_4, blue line). Also shown are the δD records from Dome C (black line; EPICA Community Members 2004) as well as from Vostok (grey line, +42 ‰; Petit *et al.* 1999). Grey shaded areas highlight interglacial periods with a Dome C δD value more than −403‰ (EPICA Community Members 2004). Marine isotope stage numbers are shown at the bottom of the figure, and all data are on the EDC2 time scale.

Wolff and Spahini, 2007